ISBN: 978-3-95450-232-5 ISSN: 2673-7000 doi:10.18429/JACoW-NAPAC2022-TUPA17

BEAM-BASED ALIGNMENT OF SEXTUPOLE FAMILIES IN THE EIC

J. C. Wang[1*], G. Hoffstaetter[1, 2], D. Sagan[1], C. Montag[2]
[1]Cornell University, Ithaca, NY, USA
[2]Brookhaven National Laboratory, Upton, NY, USA

Abstract

To steer the closed orbit in a storage ring through the center of its quadrupoles, it is important to accurately know the quadrupole centers relative to nearby beam position monitors. Usually this is achieved by beam-based alignment (BBA). Assuming the quadrupole strength can be changed individually, one finds the BPM reading where changing a quadrupole's strength does not alter the closed orbit. Since most quadrupoles are powered in series, they can only be varied independently if costly power supplies are added. For the EIC electron storage ring (ESR), we investigate whether sextupole BBA can be used instead. Individually powered sextupole BBA techniques already exist, but most sextupoles are powered in families and cannot be individually changed. We therefore developed a method where a localized bump changes the beam excursion in a single sextupole of a family, turning off all families that also have sextupoles in the bump. The bump amplitude at which the sextupole does not cause a closed orbit kick determines the sextupole's alignment. This study was made to investigate the precision to which this method can be utilized.

INTRODUCTION

The here presented Beam Based Alignment (BBA) procedure relies on the relationship between the kickers of a closed 3-bump when an active sextupole is within the bump. The strength of the kickers behind the sextupole will depend quadratically on the first kicker in order to close the bump. An example is shown in Fig. 1 where we model a very short sextupole to avoid length-effects in the analysis.

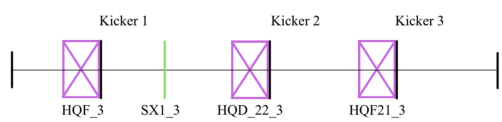

Figure 1: Diagram of a sextupole behind the first kicker of a 3-bump.

In an orbital bump with only linear elements and no sextupole magnets, the kick angles θ_2 and θ_3 provided by the second and third kicker required to close the bump are directly proportional to the bump amplitude from the first kicker θ_1. The formulas for the bump settings using optical values [2] are provided as follows:

$$\theta_2 = -\sqrt{\frac{\beta_1}{\beta_2}}\frac{\sin(\psi_3-\psi_1)}{\sin(\psi_3-\psi_2)}\theta_1$$

$$\theta_3 = \sqrt{\frac{\beta_1}{\beta_3}}\left(\frac{\sin(\psi_3-\psi_1)}{\tan(\psi_3-\psi_2)} - \cos(\psi_3-\psi_1)\right)\theta_1 \quad (1)$$

Where β represents the β-function and ψ represents the phase functions. The equations from Eq. (1) must change from linearly proportional to θ_1 to quadratic when a sextupole is added to the bump as it gives a kick angle, θ_s equivalent to:

$$\theta_s = \frac{1}{2}K_2 L(x_s - x_o)^2 \quad (2)$$

where x_o is the misalignment of the sextupole, K_2L is the integrated strength of the sextupole, and x_s is the position where the beam enters the sextupole which is linearly proportional to θ_1; θ_s then depends on θ_1^2, forcing both θ_2 and θ_3 to have a 2nd order dependence on θ_1 in order to close the bump at any bump amplitude.

The only scenario where the bump can still close using the equations from Eq. (1) is where the beam enters the sextupole directly through its center, in which case k_s would be equal to 0. If the kick strengths of the second and third kicker needed to close the bump were graphed with respect to the bump amplitude k_1, the intersection point between the quadratic curve and the linear curve for a bump with and without an active sextupole, respectively, would occur at the k_1 value needed to force the beam through the center of the sextupole as shown in Fig. 2. Because this method

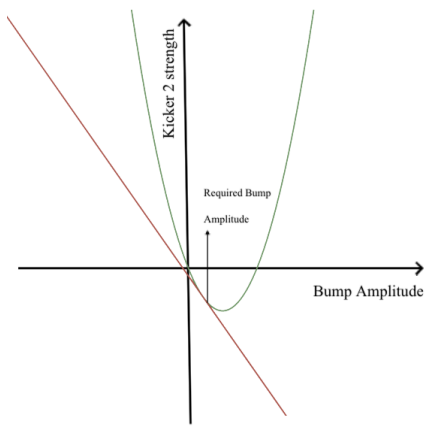

Figure 2: Graph of an example comparison between the bump settings and amplitude with and without a sextupole.

ensures that throughout the BBA procedure the bump is always closed, other nonlinear effects around the ring have

* jcw295@cornell.edu

Content from this work may be used under the terms of the CC BY 4.0 licence (© 2022). Any distribution of this work must maintain attribution to the author(s), title of the work, publisher, and DOI

ISBN: 978-3-95450-232-5 ISSN: 2673-7000 doi:10.18429/JACoW-NAPAC2022-TUPA17

no influence, as the closed orbit around the ring remains unchanged.

METHOD

The Bmad Library's Tao program [1] was used for this study. It closes the orbital bump around the sextupole back to its original orbit in an open beamline via optimization. The main focus was to observe that at different bump amplitudes, the strength of the second and third kicker depend quadratically on the first kicker, reflecting the sextupole's contribution to the angle of the beam. Two different cases were studied for this BBA method: Ideal Lattice and Lattice with Misaligned Elements. The first case has no misalignment errors, causing an initial 0 orbit before a bump is activated whereas the second case mis-aligns all the magnets on the level of 50 µm, creating an orbital distortion. For both of these cases, the BBA method's level of accuracy was tested for three orders of BPM reading errors: 0, 1 µm, and 10 µm. The following steps were applied for each case and level of error:

- Turn all sextupole families off that have a sextupole within the bump. Give kicker 1 several kick strengths that lead to bump amplitudes up to several mm and close the bump with kickers 2 and 3. This determines the linear relation $a = \theta_2/\theta_1$ and $b = \theta_3/\theta_1$. The relationship is linear, because the bump contains no sextupole strength.
- Turn the three kickers off again and activate the family of the studied sextupole as strongly as reasonable whilst keeping all families turned off that also have a sextupole in the bump. Make sure the studied family has only one sextupole within the bump. Store the closed orbit around the ring as a reference.
- Excite various bump amplitudes up to several mm. For each, close the bump so the orbit remains unchanged outside the bump region. Record the nonlinear relations $\theta_2(\theta_1)$ and $\theta_3(\theta_1)$.
- For each amplitude θ_1 repeat the process of bump closing and the resulting bump strength to increase the accuracy of θ_2 and θ_1. Here we averaged over N = 10 bump closings.
- Observe the quadratic curves and find their intersection with the linear relations obtained without sextupoles: $\theta_2(\theta_1) = a\theta_1$ and $\theta_3(\theta_1) = b\theta_1$. At the resulting bump amplitude, the orbit goes through the center of the sextupole.

Due to the small range of bump amplitudes that can reasonably be used for a bump without causing particle loss, the data, despite obeying a quadratic function, appears linear to they eye as shown in Fig. 3. To observe the quadratic behavior of the data, the linear term was subtracted from the raw data by subtracting ak_1 and bk_1 from the strength of the second and third kicker, leaving only the quadratic term that is due to the sextupole. The minimum of the quadratic curve in Fig. 4 determines the bump amplitude that leads through the sextupole center, measuring the sextupole offset.

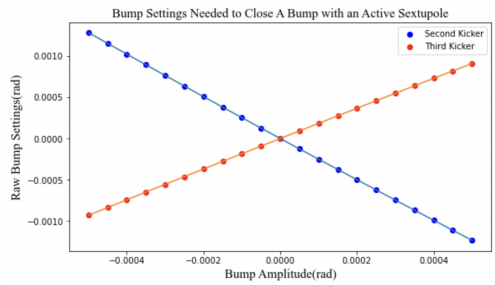

Figure 3: Raw data for the second (and third) kicker compared to the bump amplitude (Ideal Lattice). Data evaluation shows the second order components that are not visible to the eye.

Without system errors, the extremum for the second and third kicker occur at the same bump amplitude. With errors, there is a discrepancy between the extremum locations.

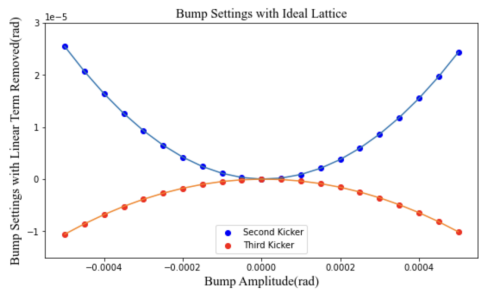

Figure 4: Fitted Adjusted data with linear term removed for the second (and third) kicker compared to the bump amplitude (Ideal Lattice).

RESULTS

Ideal Lattice

The raw and adjusted data with quadratic fits for both the second and third kicker of an Ideal Lattice after the BBA method has already been displayed in Fig. 3 and Fig. 4. No additional figures were provided for each level of BPM reading error due to looking identical with eachother.

From analytical calculations, the bump amplitude needed to perfectly force the beam through the center of sextupole in the Ideal Lattice is $\theta_1 = 56.846$ µrad.

For the simulation with no BPM reading errors, the extremum of the fits for the second and third kicker were each at $\theta_1 = 5.6846$ µrad, causing errors that were at the level of 1 pm or essentially 0 m. Significant deviations are only observed with alignment and BPM errors.

For simulations with a level of 1 µm BPM reading errors in an ideal lattice, the extremum from the second and third kicker fits were at $\theta_1 = 5.2067$ µrad and $\theta_1 = 4.6921$ µrad, respectively. This lead to a measurement error from the second kicker of 4.2 µm and from the third kicker, 8.8 µm. It can be seen that relatively realistic BPM reading errors

Content from this work may be used under the terms of the CC BY 4.0 licence (© 2022). Any distribution of this work must maintain attribution to the author(s), title of the work, publisher, and DOI

ISBN: 978-3-95450-232-5 ISSN: 2673-7000 doi:10.18429/JACoW-NAPAC2022-TUPA17

Content from this work may be used under the terms of the CC BY 4.0 licence (© 2022). Any distribution of this work must maintain attribution to the author(s), title of the work, publisher, and DOI

of 1 µm causes deterioration in the BBA method but still produces promising results.

For simulations with a level of 10 µm BPM reading errors in an ideal lattice, the extremum from the second and third kicker fits were at θ_1 = 9.3851 µrad and θ_1 = 11.331 µrad, respectively. This lead to a measurement error from the second kicker of 32.5 µm and from the third kicker, 49.1 µm. Once BPM reading errors reach the level of 10 µm, the BBA method experiences heavy deterioration in its accuracy.

Lattice with Misalignment Errors

All elements received Gaussian distributed misalignments with a sigma of 50 µm. Equation 1 leads to a bump amplitude of 0.339 31 mrad to guide the orbit through the center of the sextupole. Figure 5 shows the adjusted data with fits that display the extremum.

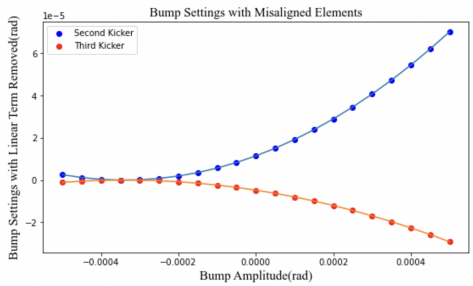

Figure 5: Second and third kicker vs. to the bump amplitude for the Lattice with Misalignments.

For no BPM reading errors, the quadratic fits had extremum at 0.339 317 mrad and 0.339 352 mrad for the second and third kicker, respectively. These bump amplitudes gave misalignment measurement errors of 0.3 µm and 0.1 µm.

For BPM reading errors at the level of 1 µm, the quadratic fits had extremum at 0.339 307 mrad and 0.339 705 mrad for the second and third kicker, respectively. These bump amplitudes gave misalignment measurement errors of 0.3 µm and 5 µm. For the lattice with misaligned magnet elements, the presence of 1 µm BPM reading errors caused less deterioration than the ideal lattice, suggesting a high level of error fluctuations when BPM reading errors are introduced.

Finally, for BPM reading errors at the level of 10 µm, the quadratic fits had extremum at 0.336 128 mrad and 0.334 284 mrad for the second and third kicker, respectively. These bump amplitudes gave misalignment measurement errors of 37 µm and 75 µm, showing a large discrepancy in the accuracy of finding the true extrema from the second and third kickers.

ERROR ANALYSIS

The goal for this Sextupole BBA method is to produce a sextupole misalignment measurement at an error level below 50 µm to be effective.

The cases of an Ideal Lattice and a Lattice with Misalignment Errors produced errors that were comparable, with the latter having lower magnitudes and consistency in accuracy as higher levels of BPM reading errors were introduced. Despite this, both cases stayed within the realm of acceptable levels of accuracy for BPM reading errors as high as 10 µm.

It should be noted that all measurements recorded in the Results section were for individual trials and the error fluctuates on a case-by-case basis. It can be seen that the case of no BPM reading errors and 1 µm BPM reading errors caused identical measurement errors in the Misaligned Elements lattice from the second kicker fit, suggesting a high level of variance when BPM noise is introduced.

It can be observed that the third kicker's quadratic fits consistently produced less accurate bump amplitude extremum than the second kicker's. This is likely due the third kicker's role of adjusting the change in angle caused by the first and second kicker, propagating any errors from the second kicker into the third kicker. Therefore, for the most accurate sextupole measurement readings, only the fit from the second kicker should be considered.

These errors were minimized by closing the bump with M = 83 BPM readings and averaging over N = 10 bump closings. For a closed orbit, a higher number of BPMs, M, could be used which could even further decrease the influence of BPM reading errors on the measurement accuracy. For these simulations done in an open beamline, M was limited.

Further errors that were not yet investigated in the scope of this experiment include magnet strength errors and the propagation of error from not fully closing a bump due to BPM errors in a closed orbit.

CONCLUSIONS

Modern Sextupole BBA techniques involving the influence of the sextupole on the beam's orbit and the β-functions exist but deteriorate in accuracy when sextupoles are powered in families. The here presented Sextupole BBA technique involving the study of an orbital bump through one member of a sextupole family was simulated. In an ideal simulation it determines the offset of a sextupole to machine precision. However, in a real ring with misalignments and BPM errors, this BBA method the sextupole alignment can only be determined with limited precision. Specifically, random BPM errors lead to errors in the bump closure, limiting what can be concluded about kicks in the sextupole. In this study we analyze BPM errors as high as 10 µm, a realistic number for modern instrumentation, for both a zero-orbit Ideal Lattice and non-zero distorted orbit lattice with misaligned BPMs. The Sextupole alignment can be determined with uncertainty at the level of 30 µm, showing potential for utilization in the actual ESR ring and other rings with sextupole families. While this study focused on the ability to perform this BBA method in an open beamline for simplicity and analytical understanding, future studies involving closed orbits will be conducted to analyze the accuracy of this method in a ring with periodic closed orbit.

ISBN: 978-3-95450-232-5 ISSN: 2673-7000 doi:10.18429/JACoW-NAPAC2022-TUPA17

REFERENCES

[1] Tao Program, https://www.classe.cornell.edu/bmad/tao.html

[2] K. Wille, "Local orbit bumps", in *The physics of particle accelerators: An introduction*, NY, USA: Oxford University Press, 2013, pp. 127–135.

Content from this work may be used under the terms of the CC BY 4.0 licence (© 2022). Any distribution of this work must maintain attribution to the author(s), title of the work, publisher, and DOI